SUPPLEMENTARY FIGURE LEGENDS

Figure S1. Bioinformatics workflow for analysis of 3' UTR lengths of human protein-coding transcripts obtained from GENCODE Release 47 (October 2024). Annotated 3' UTRs were divided into six groups according to their length. Their sizes are written in the lower right corner of the corresponding boxes. Each of the groups was also divided into three inner groups according to the stop codon type — thus getting a total of 24 groups (with and without stop codon disaggregation) that were next used for GO and KEGG over-representation analysis (ORA). Isoform expression data were obtained from the Adult GTEx database (Analysis V10).

Figure S2. Results of GO ORA compareCluster analysis. Each circle represents the over-represented gene ontology category specified on the Y-axis within the analysis group specified on the X-axis. The color and size of the circle reflect the adjusted p-value and gene ratio, respectively.

Figure S3. Results of KEGG ORA compareCluster analysis. Each circle represents the over-represented KEGG pathway on the Y-axis within the analysis group specified on the X-axis. The color and size of the circle reflect the adjusted p-value and gene ratio, respectively.

Figure S4. (**A**) Distribution of 3′ UTR lengths of transcripts corresponding to the genes associated with cytoplasmic translation and over-represented in the groups «11-30» and «31-150» according to the GO ORA results. It depicts that it is more likely for UAA transcripts to have smaller 3'UTRs in that GO category. (**B**) Isoform expression as a function of 3′ UTR length. Expression is estimated as total transcripts per million (sum(TPM)). Colors represent different groups based on 3′ UTR length. GENCODE – whole dataset of human protein-coding transcripts with annotated 3′ UTRs; MANE Select – subset of main isoforms from MANE Select. **(C)** Relative expression of transcripts with different 3′ UTR lengths in different tissues. Colors represent different groups based on 3′ UTR length.

Figure S5. Influence of 3′ UTR lengths on translation rate in nuclease-treated lysates. (**A**) Titration curves of model mRNA with long synthetic 3' UTR (168 nt) in different lysates. (**B**) Rates of translation of mRNAs containing different 3' UTRs and poly(A) tails in RRL and WGE. Maximum translation rate v_0 is in relative luminescent units per minute (RLU/min). Data are presented as mean ± standard error (n = 3). Asterisks indicate statistically significant differences compared to the corresponding 0 nt control (*, $p < 0.05$; **, $p < 0.01$). Non-significant differences are not shown.

Figure S6. Longer 3′ UTRs increase the stability of non-adenylated mRNA. The relative stability (3′-end / internal amplicon ratio, $2^{-\Delta Ct)}$), of model mRNAs containing synthetic 3′ UTRs of varying lengths, with or without poly(A) tail, was measured in HEK293T lysate (**A**) and RRL (**B**). Data are presented as mean ± standard error (n = 5). Asterisks indicate statistically significant differences compared to the corresponding 0 nt control (*, $p < 0.05$; **, $p < 0.01$; ***, $p < 0.001$). Non-significant differences are not shown.

Figure S7. Structural characteristics of 3′ UTRs used in the study. (A, B) Fragment analysis of 3′ UTRs using FAM-labeled reverse primers specific for the GAPDH 3′ UTR (**A**) and the synthetic 3′ UTR (**B**). Efficiency of cDNA synthesis is indicated by relative fluorescence units (RFU). (**C-E**) RNase V digestion

analysis of 3'UTRs. (**C**) Agarose gel electrophoresis of synthetic and GAPDH 3′ UTRs incubated with increasing dilutions of RNase V. (**D**) Agarose gel electrophoresis of tRNA and synthetic 3′ UTR incubated with increasing dilutions of RNase V. tRNA, which contains stable double-stranded stems, served as a positive control for RNase V activity. (**E**) Agarose gel electrophoresis of unstructured CA-repeat, GAPDH 3′ UTR and synthetic 3′ UTR incubated with increasing dilutions of RNase V. The CA-repeat RNA was used as a negative control for RNase V cleavage.

Figure S8. (**A**) Gel-shift analysis of fluorescently labeled ASO or RSO binding to non-adenylated and polyadenylated Nluc mRNAs. Duplexes formed between mRNA and ASO are indicated as 'mRNA*ASO'. (**B**) Titration of ASO in peptide release suppression assay using preTC-Nluc(UAA) assembled on polyadenylated mRNA with synthetic 3' UTR. (**C**) Western blot analysis of purified preTCs-Nuc assembled on polyadenylated mRNAs containing different stop codons and varying lengths of the synthetic 3'UTR. Membranes were probed with antibodies against PABP and ribosomal protein rpL9 (loading control). (**D**) Rates of peptide release induced by different amounts of human eRF1-eRF3a or eRF1 at preTC-Nluc, assembled at polyadenylated mRNA with UAA stop codon and 168 nt 3′ UTR.

Figure S9. Effect of 3'UTR length on peptide release rate at UGA stop codon in reconstituted translation system. (**A**) Schematic representation of model mRNAs encoding MVHL peptide and containing different lengths of synthetic 3'UTR, used to determine peptide release rate in reconstituted translation system. (**B**) Relative rates of peptide release induced by human eRF1-eRF3a in the presence or absence of PABP at preTCs-MVHL, assembled at polyadenylated mRNAs with UGA stop codon and 3'UTRs. (**C**) Relative rates of peptide release induced by Ea-eRF1-eRF3a or Bj-eRF1 in the presence or absence of PABP at preTCs-MVHL, assembled at polyadenylated mRNAs with UGA stop codon and 3'UTRs. Brackets indicate the order of addition of release factors and PABP to preTC. Rate of peptide release v_0 on preTC-MVHL is in count per minute (cpm) of a fraction of released radioactively labeled tetrapeptide. Data are presented as mean ± standard error (n = 3). Asterisks indicate statistically significant differences compared to the corresponding 0 nt control (*, $p < 0.05$; **, $p < 0.01$). Non-significant differences are not shown.

Figure S10. (**A**) Alignment of the eRF1 N-domain from studied species. Red-boxed regions indicate conserved motifs required for stop codon recognition by eRF1. Numbering is based on the human sequence. Blue-shaded areas highlight substitutions compared to the human sequence. (**B**) Schematic representation of model chimeric eRF1 containing N domains of *E. aediculatus* or *B. japonicum* eRF1 and MC domain of human eRF1 and specificity of ciliates eRF1s, and specificity of ciliate eRF1s to stop codons (UGA codon in these species is recognized as cysteine or tryptophan codon). (**C**) Ability of human and chimeric eRF1s to form post-termination complexes at the UGA stop codon determined by fluorescent toe-print assay in reconstituted mammalian translation system.

Figure S11. Optimization of factors concentrations for competition between eRF1 and *Bn*-Trp-tRNA^{Trp} at the UGA stop codon. (**A**) Rates of peptide release induced by different concentrations of human eRF1-eRF3a at preTC-Nluc, assembled at polyadenylated mRNA with UGA stop codon and 168 nt 3′ UTR. (**B**) Rates of peptide release induced by 6 nM human eRF1-eRF3a and different concentrations of eEF1a at preTC-Nluc, assembled at polyadenylated mRNA with UGA stop codon and 30 nt 3′ UTR. (**C**) Rates of peptide release induced by 6 nM human eRF1-eRF3a and 10 nM human eEF1A in the presence

of increasing concentrations (0 – 200 nM) of either mut 5-bp tRNA or wt 4-bp tRNA at preTC-Nluc assembled on polyadenylated mRNA with UGA stop codon and 30 nt 3′ UTR. This titration demonstrates that a high concentration of tRNA (200 nM) is required to detect weak suppression of eRF1 activity by the suppressor tRNA. Maximum translation termination rate v_0 is expressed in relative luminescent units per minute (RLU/min).

SUPPLEMENTARY TABLE

Table S1. Primers and oligonucleotides

name	**sequence**
5’RT-PCR_R	AGTGCAGGATCACCTTAAAGTGAT
5’RT-PCR_F	AACCTGGACCAAGTCCTTGAAC
ASO	AACTTGTTTATTGCAGCTTATAATGGTTACAAATAAAGCAATAGCATCAC
ble_for_external	ATGGAAGGAGACGAGCTTACTCAGAATATCGAGCAGTGGAAAATAAAGCGACTGATTGATAATCTGGACAAAGCCCGTGGAAATGGGACATCCCTGATCTCACTGATCATCCCTCCTCGAGAGCA
ble_for_internal	ATCATCCCTCCTCGAGAGCAGTTGCCCATCATCAACAAGATGATCACTGAAGAATATGGAAAGTCATCTAACATCAAATCAAGAATCGTCAGACAGGCTGTTCAAAGTGCTCTCACCTCCACAAAAGAGC
ble_rev_internal	TATACTTTTTCTCGCAGACTCCTTCTTCGTTGATAACTTCGCCACAATACAGAATTAGACCGTTTGCTGGGAGCCTATTATTATAAAGTTTGAGACGCTCTTTTGTGGAGGTGAGA
ble_rev_external	ATCCATGACCAGAAGATCTTTAAGTGGCTGTGTGTGGAATTTATTATCGCAAATATAAAGAGTGGTATTGATGGCTCGGTATGGCTGGAAGTCAATCGTATACTTTTTCTCGCAGACTC
eu_for_external	ATGTCAGTTCTTGATAGCAATGTTGAGACCTGGAAGATCAAGAGACTTATTAAAAACCTTGAGAAGTTGAGAGGAAATGGAACCAGCATGATTTCTTTATTGTTATCGCCAAGGGATCA
eu_for_internal	TTGTTATCGCCAAGGGATCAGATTTCAAAAGTACAGGGAATGCTCGCAGGAGAAGCAGGTACCGCAGTTAATATTAAATCAAGAGTAAATCGTTTGGCAGTTCTTAGTGCTATCACATCT
eu_rev_internal	ACTTCTTCTCAGAGCCGTCTTCACCAATAACTGTTCCACAATAAACTACAAGTCCATTATTGGGTGTTCTGGTATATAACTTTAGTCTTTCTTTAGCAGATGTGATAGCACTAAGAA
eu_rev_external	AAGTTCAAAAAGAGGCTCAGTGCAGAATTTATTGTCACAGATATATTTGAACGTGTTTAATGGTCTGAATGGTTCAAAGTCAATAGTATACTTCTTCTCAGAGCCGTCT
FAM-toe	[6-FAM]-GCATGTGCAGAGGACAGG
Fluc_3UTR_F_GB	CGCATTCTGGCGTAAAATGTAACTGTATTCAGCGAT
Fluc_3UTR_F_GB(UAG)	CGCATTCTGGCGTAGAATGTAACTGTATTCAGCGAT
Fluc_3UTR_F_GB(UGA)	CGCATTCTGGCGTGAAATGTAACTGTATTCAGCGAT
Fluc_3UTR_R_gb	gtatcttattgtctgctcgAGTTGGGTAACGCCAGG
Fluc_R_10	TTTTTTTTTTTTTTTTTTTTTTTTTTTTTTTTTTTTTTTTTTTTTTTTcagttacatt
Fluc_R_30	TTTTTTTTTTTTTTTTTTTTTTTTTTTTTTTTTTTTTTTTTTTTTTTTaatttcgtcatcgctgaatacagtt
globin_rev	TCAGTGGTATTTGTG

globin-A50_rev	TTTTTTTTTTTTTTTTTTTTTTTTTTTTTTTTTTTTTTTTTTTTTTTTTTCAGTGGTATTTGTG
LucA50_R	TTTTTTTTTTTTTTTTTTTTTTTTTTTTTTTTTTTTTTTTTTTTTTTTTTagttgggtaacgccag
MVHL-3UTR-0-UGA_R	TTTTTTTTTTTTTTTTTTTTTTTTTTTTTTTTTTTTTTTTTTTTTTTTTTCACAGATGCACCATTCTGTCTGTTTTGGGGGA
MVHL-3UTR-10-UGA_R	TTTTTTTTTTTTTTTTTTTTTTTTTTTTTTTTTTTTTTTTTTTTTTTTTTCTCCACACATcACAGATGCAC
MVHL-3UTR-30_R	TTTTTTTTTTTTTTTTTTTTTTTTTTTTTTTTTTTTTTTTTTTTTTTTTTCAGGGCAGTGACCGCA
MCdom eRF1_petSUMO_F	TTTGGATTCATTGTAATAGATGGTAGTGGTGC
MCdom petSUMO_eRF1_R	CCGAATAAATACCTAAGCTCTAGTAGTCATCAAGGTCAAAAA
Nluc_R_ML	TTACGCCAGAATGCGTTCG
Nluc_R_ML (UAG)	CTACGCCAGAATGCGTTCG
Nluc_R_ML(UGA)	TCACGCCAGAATGCGTTCG
Nluc_F_ML	CGAGCAGACAATAAGATACATTGAT
petSUMO_ble_R	CCATCTATTACAATGAATCCAAAGTCGACATCCATGACCAGAAGATC
petSUMO_eRF1_bj	GAGAACAGATTGGTGGTATGGAAGGAGACGAGCTTACTCA
petSUMO_eRF1_euplotes	GAGAACAGATTGGTGGTATGTCAGTTCTTGATAGCAATGTT
petSUMO_eu_R	CCATCTATTACAATGAATCCAAAAAGTTCAAAAAGAGGCTCAGT
petSUMO_F	AGCTTAGGTATTTATTCGGCGCAAAGTG
petSUMO_R	ACCACCAATCTGTTCTCTGTGAGC
pNL_3'_10	AGTCGCGGCC
pNL_3’_30	GCCGGCCGCCCCGA
pNL_3’_168	AACTTGTTTATTGCAGCTTATAATGG
pNL_3'_10_A50	TTTTTTTTTTTTTTTTTTTTTTTTTTTTTTTTTTTTTTTTTTTTTTTTTAGTCGCGGC
pNL_3’_30_A50	TTTTTTTTTTTTTTTTTTTTTTTTTTTTTTTTTTTTTTTTTTTTTTTTTGCCGGCCGCCCCGA
pNL_3’_168_A50	TTTTTTTTTTTTTTTTTTTTTTTTTTTTTTTTTTTTTTTTTTTTTTTTTAACTTGTTTATTGCAGCTTATAATGG
pNL_UAA_3'_0_A50	TTTTTTTTTTTTTTTTTTTTTTTTTTTTTTTTTTTTTTTTTTTTTTTTTTACGCCAGAATGCGTTCG
pNL_UAA_3’_0	TTACGCCAGAATGCGTTCG
pNL_UAG_3'_0_A50	TTTTTTTTTTTTTTTTTTTTTTTTTTTTTTTTTTTTTTTTTTTTTTTTTcTACGCCAGAATGCGTTCG

pNL_UAG_3’_0	CTACGCCAGAATGCGTTCG
pNL_UGA_3'_0_A50	TTTTTTTTTTTTTTTTTTTTTTTTTTTTTTTTTTTTTTTTTTTTTTTTTTTCACGCCAGAATGCGTTCG
pNL_UGA_3’_0	TCACGCCAGAATGCGTTCG
RSO	TGGCCGGAAATGGTACGGATGTAATAAGCGTGGATAAAAAAGTAATTAGA
RT-FW Nluc	TGGCACACTGGTAATCGAC
RV3L	CTAGCAAAATAGGCTGTCCCCAG
T7prom-globinF	CTAATACGACTCACTATAGGGGCACAAATACCACTG
tRNAW(CCA)4bp_F	GCAGCTAATACGACTCACTATAGGGGGCTTAGCTCAGTGGCAGAGTACTGGATTCCAAATC
tRNAW(CCA)4bp_U42G5bp_R	tggTGAGGACTACAGGAATTGAACCTGCGACCCCTGGATTTGGAATCCAGTACTCTGCCACT
tRNAW(CCA)4bp_wt_R	tggTGAGGACTACAGGAATTGAACCTGCGACCCATGGATTTGGAATCCAGTACTCTGCCACT

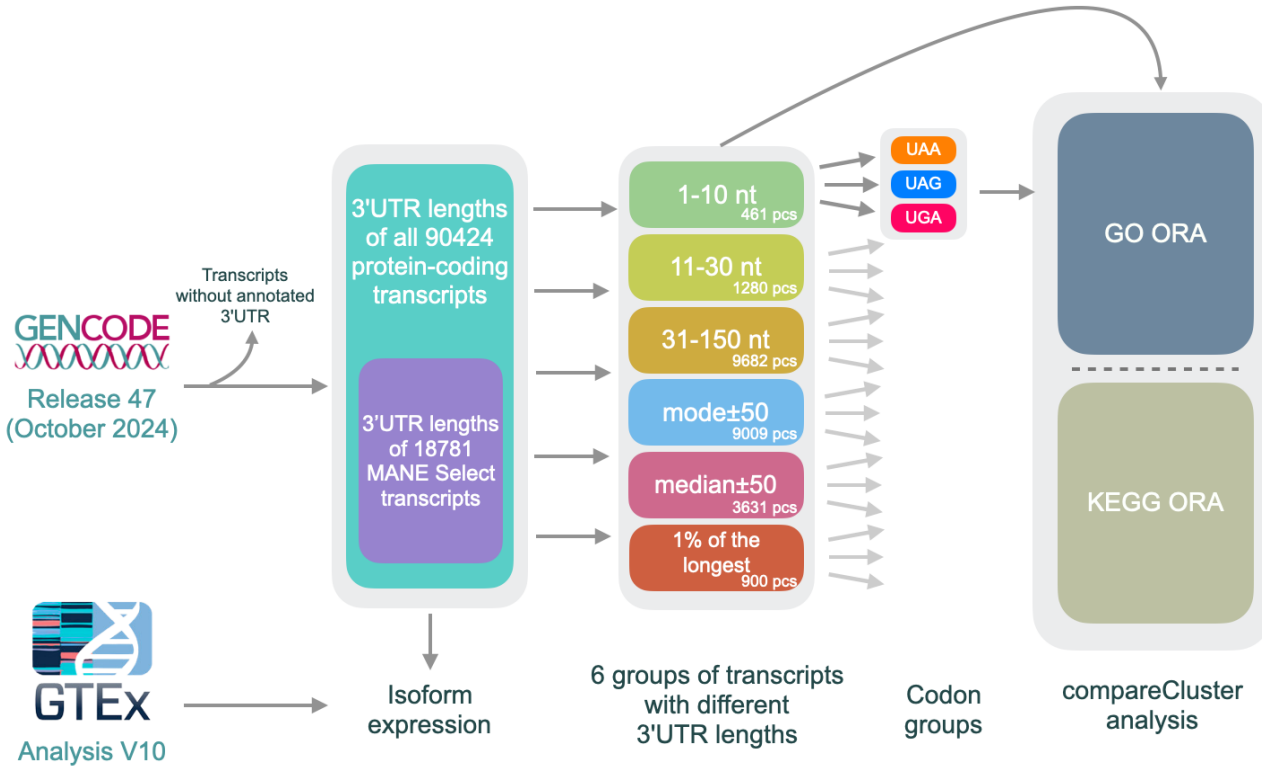
GENCODE
Release 47
(October 2024)
Transcripts
without annotated
3'UTR
3'UTR lengths
of all 90424
protein-coding
transcripts
3'UTR lengths
of 18781
MANE Select
transcripts
GTEx
Analysis V10
Isoform
expression
1-10 nt
461 pcs
11-30 nt
1280 pcs
31-150 nt
9682 pcs
mode±50
9009 pcs
median±50
3631 pcs
1% of the
longest
900 pcs
6 groups of transcripts
with different
3'UTR lengths
UAA
UAG
UGA
Codon
groups
GO ORA
KEGG ORA
compareCluster
analysis

Fig. S1

GO GENCODE Fig. S2

KEGG GENCODE Fig. S3

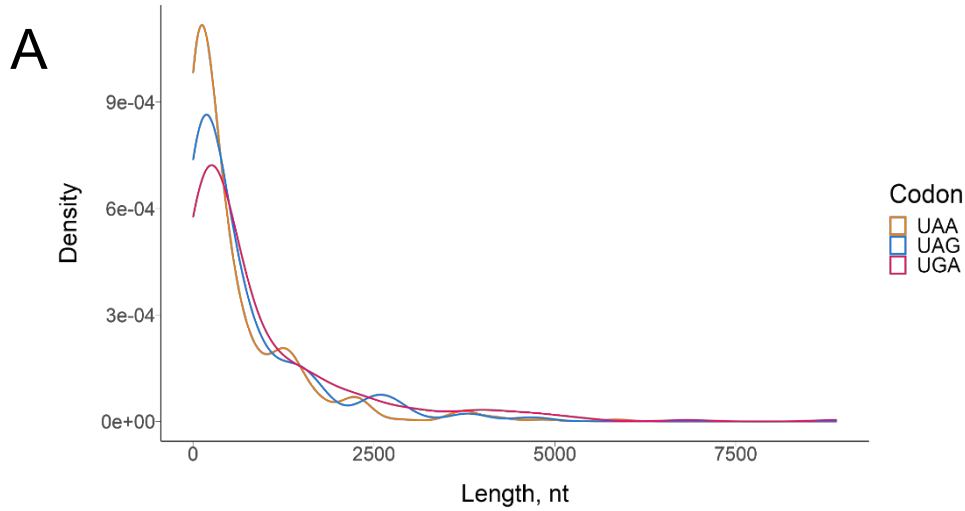
A
Density
9e-04
6e-04
3e-04
0e+00
0
2500
5000
7500
Length, nt
Codon
UAA
UAG
UGA

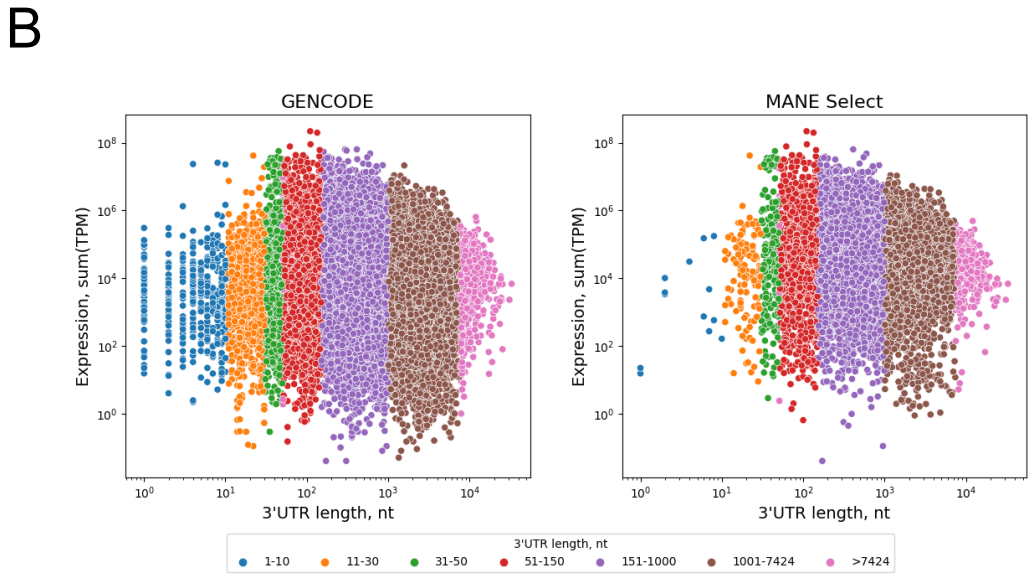
B
GENCODE
MANE Select
Expression, sum(TPM)
3'UTR length, nt
3'UTR length, nt
1-10
11-30
31-50
51-150
151-1000
1001-7424
>7424

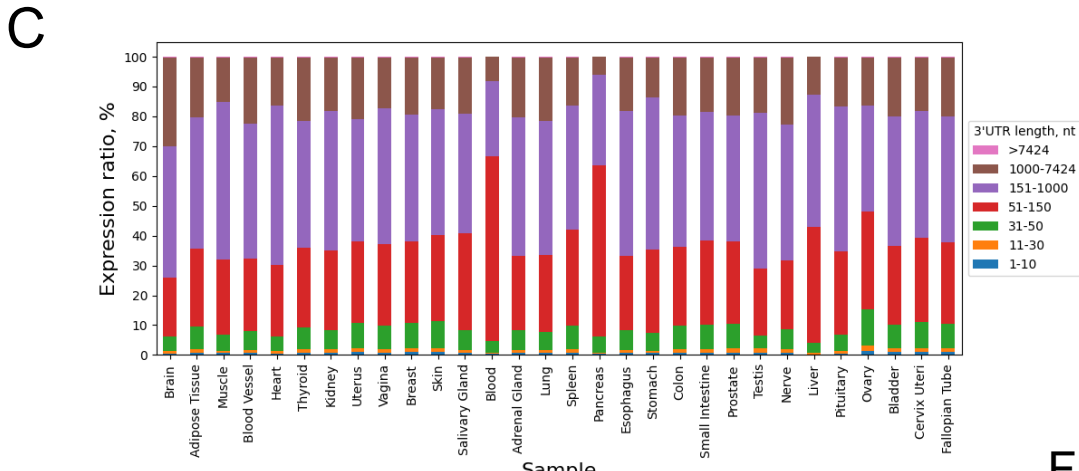
C
Expression ratio, %
Sample
Brain
Adipose Tissue
Muscle
Blood Vessel
Heart
Thyroid
Kidney
Uterus
Vagina
Breast
Skin
Salivary Gland
Blood
Adrenal Gland
Lung
Spleen
Pancreas
Esophagus
Stomach
Colon
Small Intestine
Prostate
Testis
Nerve
Liver
Pituitary
Ovary
Bladder
Cervix Uteri
Fallopian Tube
3'UTR length, nt
>7424
1000-7424
151-1000
51-150
31-50
11-30
1-10

Fig. S4

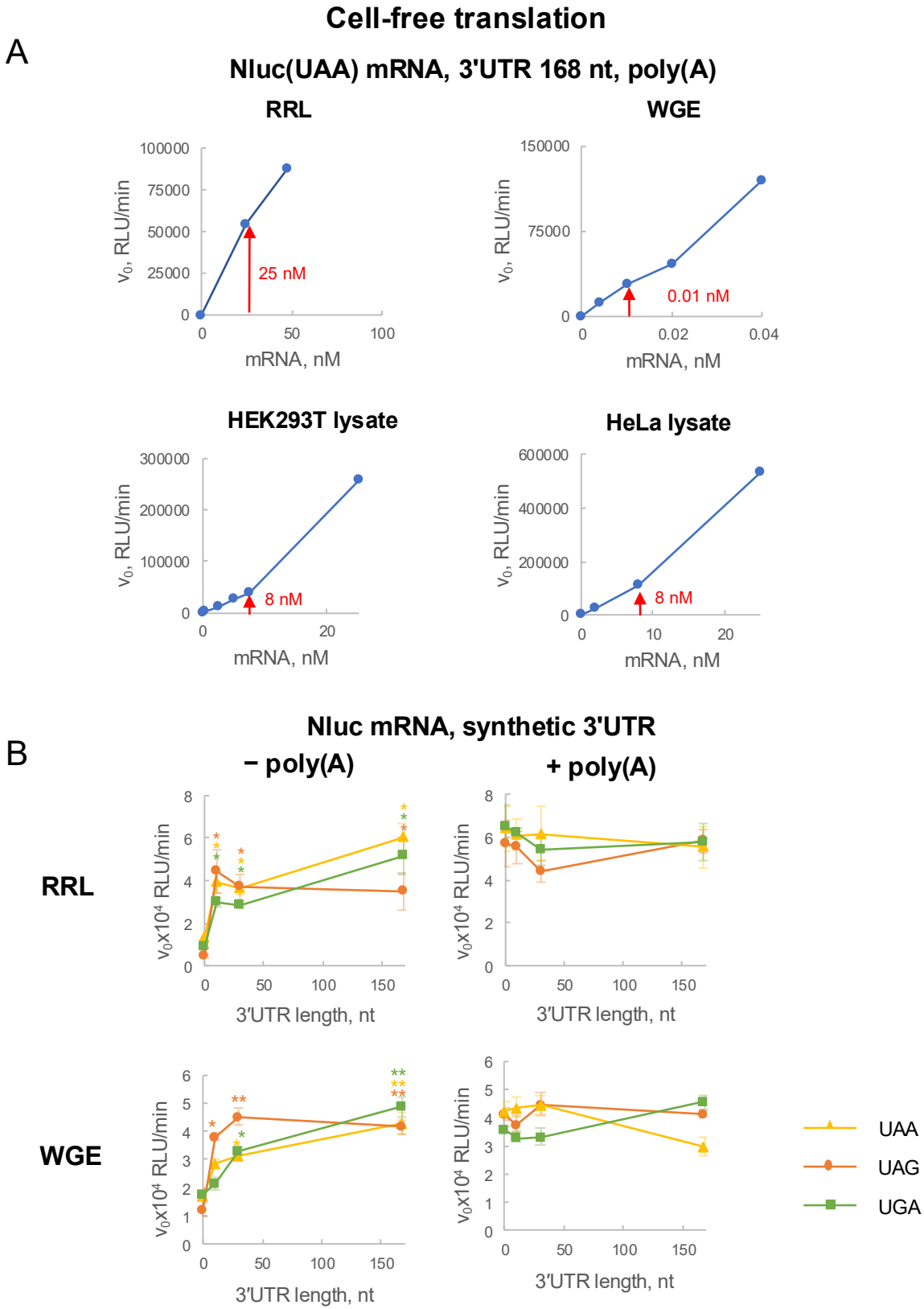
Cell-free translation
A
Nluc(UAA) mRNA, 3'UTR 168 nt, poly(A)
RRL
WGE
HEK293T lysate
HeLa lysate
v0, RLU/min
mRNA, nM
25 nM
0.01 nM
8 nM
8 nM
B
Nluc mRNA, synthetic 3'UTR
− poly(A)
+ poly(A)
RRL
WGE
v0x10^4 RLU/min
3′UTR length, nt
UAA
UAG
UGA

Fig. S5

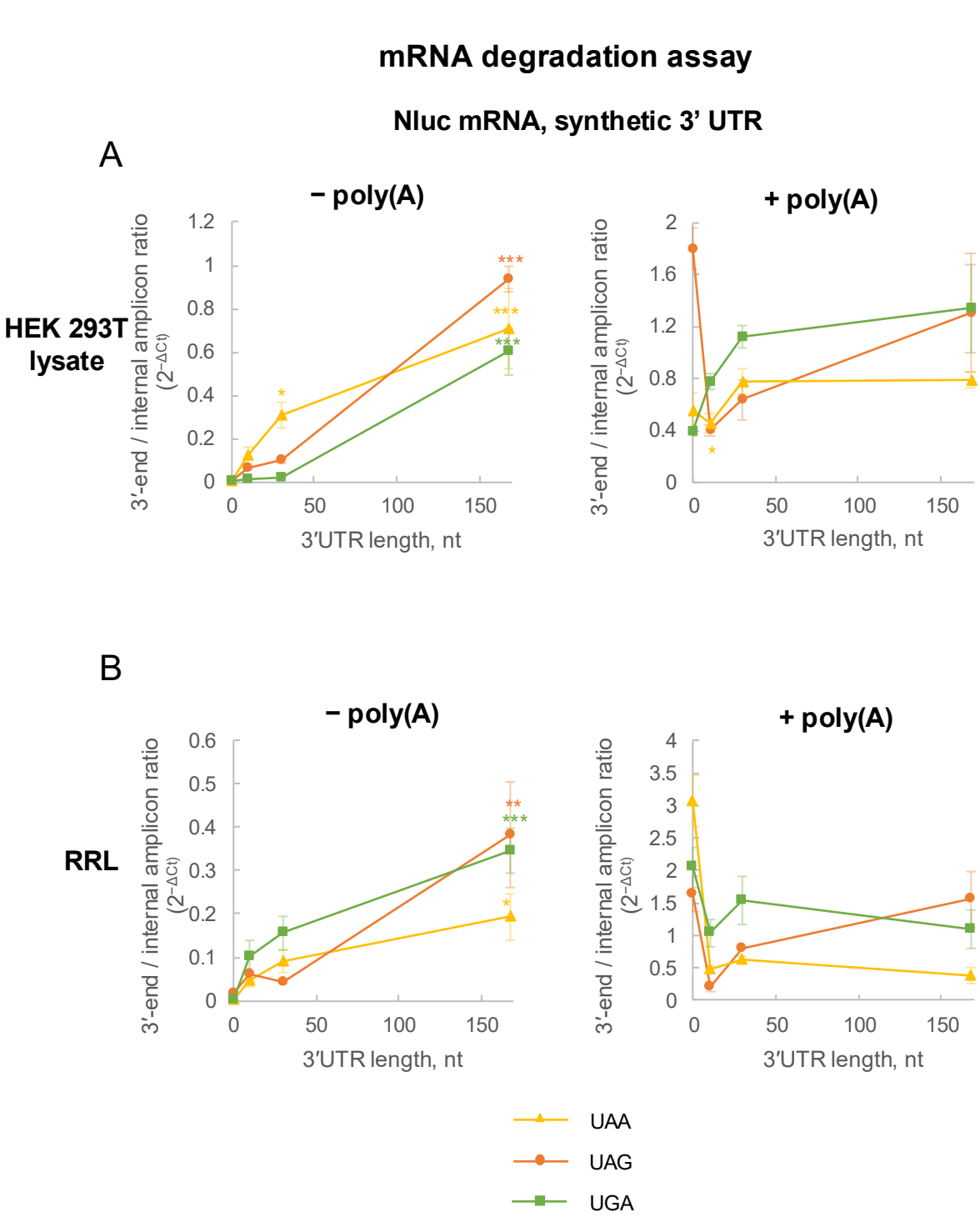
mRNA degradation assay
Nluc mRNA, synthetic 3' UTR
A
HEK 293T lysate
− poly(A)
+ poly(A)
3′-end / internal amplicon ratio (2^−ΔCt)
3′UTR length, nt
B
RRL
UAA
UAG
UGA

Fig. S6

Fragment analysis of 3'UTRs

A

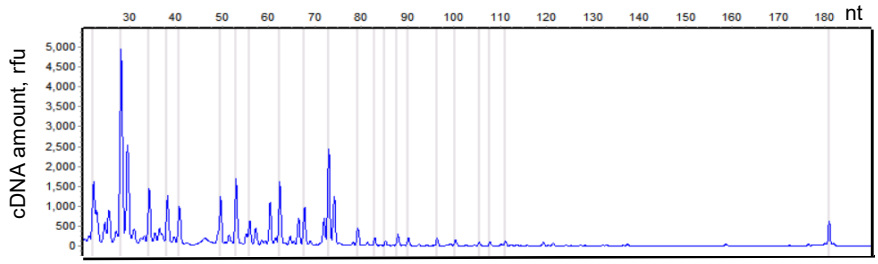

GAPDH 3'UTR

B

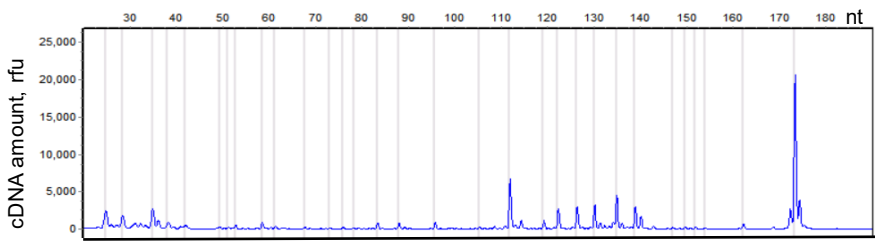

Synthetic 3'UTR

RNase V analysis of 3'UTRs

C

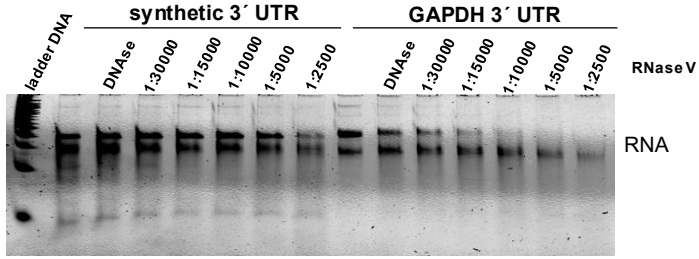

D

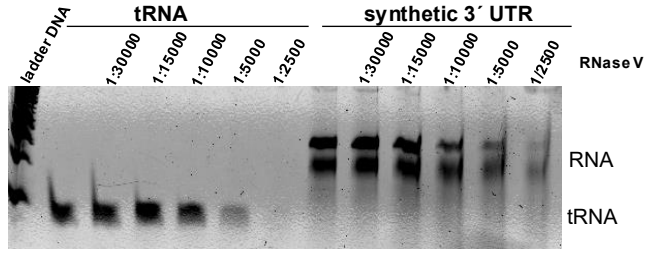

E

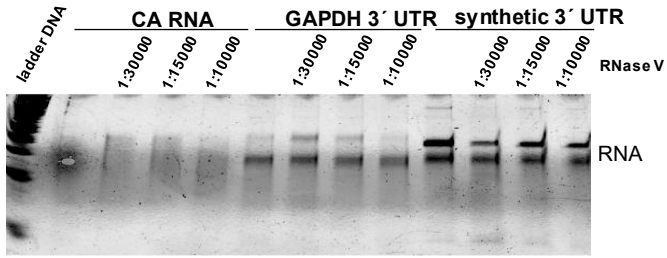

Fig. S7

A

ASO binding assay

FAM

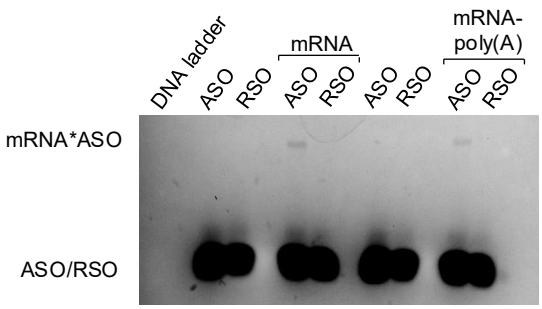

Ethidium bromide

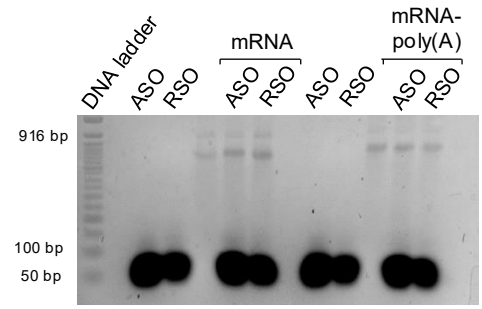

B

Peptide release assay

preTC-Nluc(UAA), 168 nt 3' UTR, poly(A)

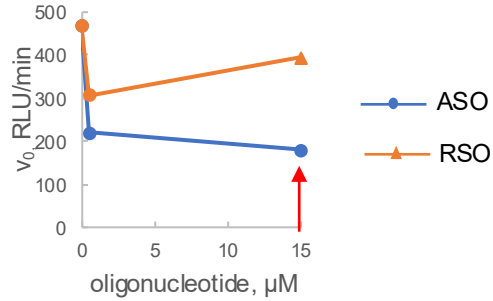

C

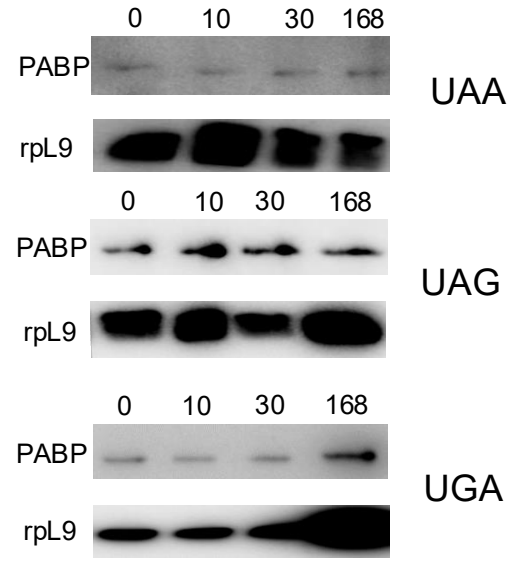

D

Peptide release assay

preTC-Nluc(UAA), 3' UTR 168 nt, poly(A)

eRF1 + eRF3a

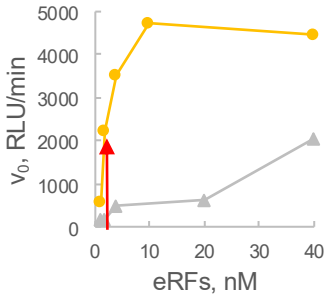

eRF1

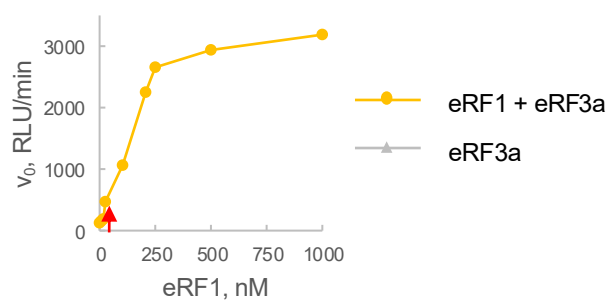

Fig. S8

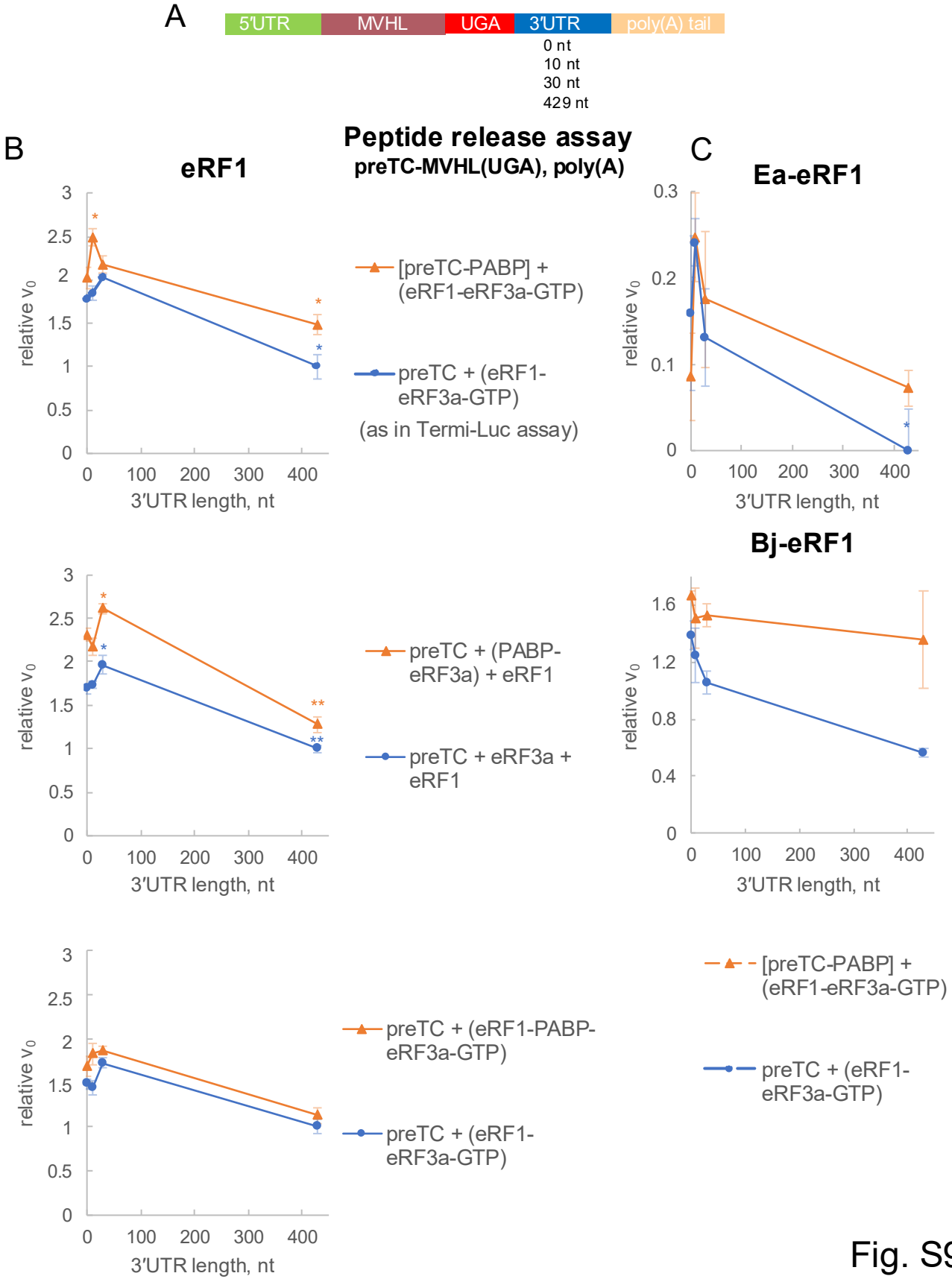
A
5′UTR
MVHL
UGA
3′UTR
poly(A) tail
0 nt
10 nt
30 nt
429 nt
B
Peptide release assay
preTC-MVHL(UGA), poly(A)
eRF1
relative v0
3′UTR length, nt
[preTC-PABP] + (eRF1-eRF3a-GTP)
preTC + (eRF1-eRF3a-GTP)
(as in Termi-Luc assay)
preTC + (PABP-eRF3a) + eRF1
preTC + eRF3a + eRF1
preTC + (eRF1-PABP-eRF3a-GTP)
preTC + (eRF1-eRF3a-GTP)
C
Ea-eRF1
Bj-eRF1
[preTC-PABP] + (eRF1-eRF3a-GTP)
preTC + (eRF1-eRF3a-GTP)

Fig. S9

A

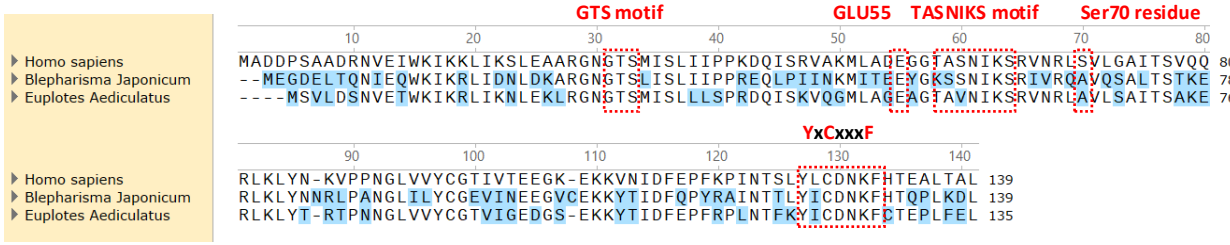

B

ciliate sequence

human sequence

	UAA	UAG	UGA
Hs-eRF1	STOP	STOP	STOP
Ea-eRF1	STOP	STOP	Cys
Bj-eRF1	STOP	STOP	Trp

C

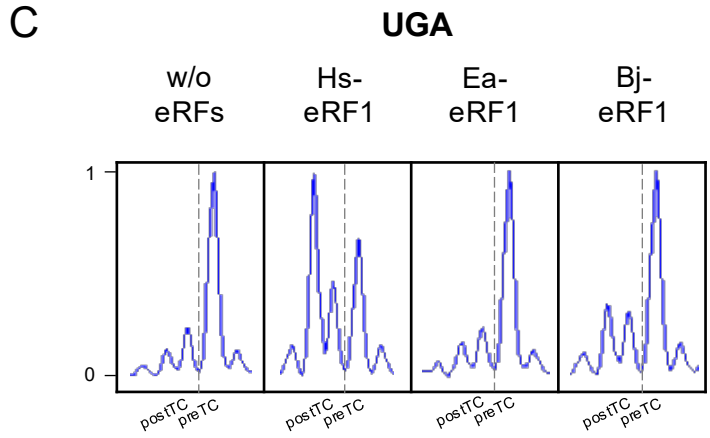

Fig. S10

Peptide release assay

preTC-Nluc(UGA), poly(A)

A

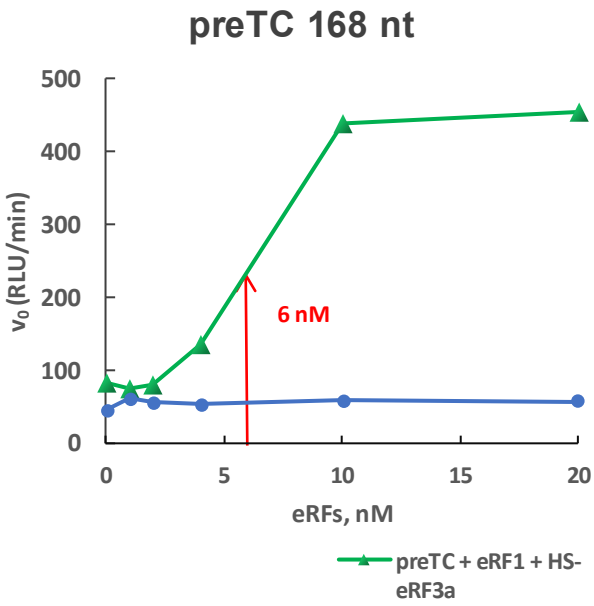

B

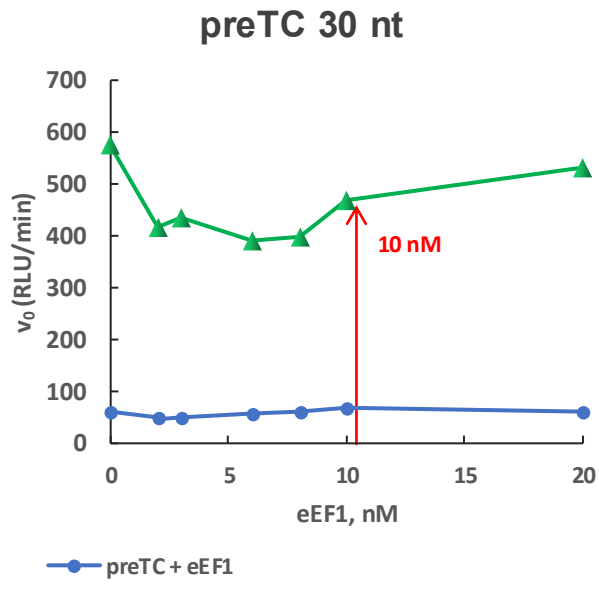

C

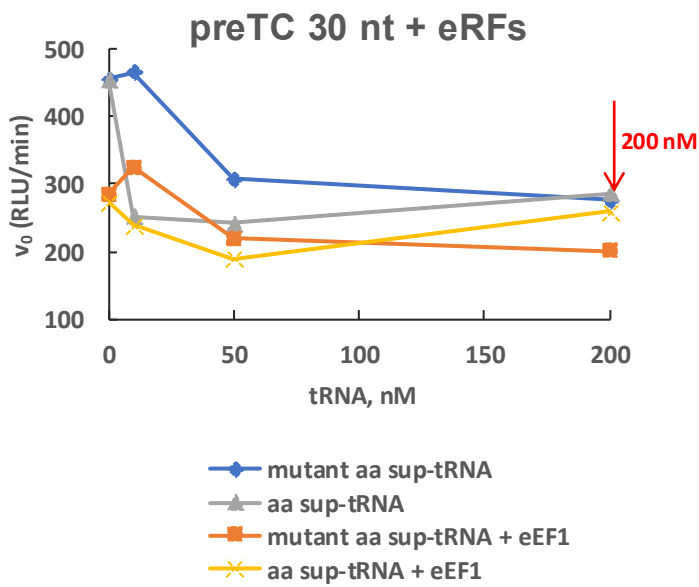

Fig. S11